Hindawi
Advances in Civil Engineering
Volume 2018, Article ID 6238910, 14 pages
https://doi.org/10.1155/2018/6238910

Research Article

Comparative Analysis of Roadway Reinforcement Effects Based on Fluid-Solid Coupling in the Fractured Zone of Water-Rich Fault

Jihua Zhang,[1] Yun Dong,[1] Yadong Chen,[1] Yang Jiang,[1] Huasheng Sun,[1] Yuqing Fan,[2] and Chun Wang[3]

[1]*Faculty of Architecture and Civil Engineering, Huaiyin Institute of Technology, Huai'an, Jiangsu 223001, China*
[2]*School of Mining Engineering, Guizhou University of Engineering Science, Bijie, Guizhou 551700, China*
[3]*Shanxi Coal Transportation and Sales Group Jincheng, Jincheng, Shanxi 048000, China*

Correspondence should be addressed to Yun Dong; hadyun@163.com

Received 3 April 2018; Revised 20 July 2018; Accepted 31 July 2018; Published 6 September 2018

Academic Editor: Dengke Wang

Copyright © 2018 Jihua Zhang et al. This is an open access article distributed under the Creative Commons Attribution License, which permits unrestricted use, distribution, and reproduction in any medium, provided the original work is properly cited.

Water inrush is a common geological disaster during the roadway excavation process in the broken zone of water-rich faults. In this paper, the 15107 mining roadway built by Yuxing coal mine in such a fault zone was used as a case study to determine the water content of the surrounding rocks and a fault zone using the transient electromagnetic method (TEM). Also, the mechanics characteristics of such rocks in both saturated and unsaturated states were analyzed, a computational model for fluid-solid coupling in the water-rich fault fracture zone was established, and the permeability coefficient of the rocks under both shield support and bolt-grouting support was compared, along with analyzing the changes in pore pressure, fissure water velocity, and characteristics of deformation in the surrounding rocks. The numerical simulation results show that the fault range has an influence of about 20 m, which causes the forms of permeability coefficient to change like a hump. The permeability coefficient in the fractured zone is the largest, and the mutation rate at the fault plane is faster. Bolting not only reduces the permeability coefficient of the surrounding rock that is 1/10 of the beam support but also prevents the roof fissure water inrushing the roadway and the surrounding rock of the floor, while also causing the pore-water pressure to decrease, even reduce to zero, in front of the working face and floor. The flow velocity of the fissure water can be decreased by bolting, which can effectively control the deformation of the surrounding rock by 38.7%~65% compared with the shield support. The practice results show that this method can effectively recover the cracks surrounding the mining roadway and stop gushing water. Concurrently, it successfully controls deformation of the surrounding rocks in the fault zone, thus ensuring stability of the roadway and facilitating safer mining production.

1. Introduction

As an important energy source, coal shoulders the important task of safeguarding national economy and social development [1]. With the increase of mining depth and strength, the geological conditions of coal mining become more complicated, and mine accidents such as water inrush, roof collapse, and rock burst often occur, which seriously threaten safe and efficient production of coal mine and the safety of miner's life and property [2, 3]. Mine water inrushing is one of the main geological disasters often encountered in coal mining and is also an important factor restricting sustainable development of most mining areas. According to statistics, there have been over 200 flooded well accidents in China in the last 30 years [4]. The main factors inducing a water inrush are related to the geological structure. Preexisting faults are important water conduits, and ~80% of the large water inrush disasters that cost more than one million Yuan in northern China were caused by karst water inrush through fracture zones, while the remaining 20% were related to mining-induced fissures [5].

The groundwater in a water-rich fault intrudes into the roadway, the surrounding rock through the dynamic development of fissures. Also, through physical and chemical interactions with the rock minerals in the surrounding rock of the mining site, rock strength is continuously attenuated, and the bearing capacity of the surrounding rock also decreases, thereby inducing deformation along roadways, working site, and other surrounding rocks. In particular, swelling soft rock absorbs water and causes large deformation in a soft rock tunnel, causing collapses in severe cases and being a serious threat to coal mining [6].

Grouting is the main initiative to support the roadway and is also the most effective method to control water. Grout has the ability to block water, increase the strength of the surrounding rock, and enhance the resistance to deformation of the surrounding rock. Much research has been conducted on grouting technology and its application [7]. Wang et al. [8, 9] implemented a bolt-grouting supporting system with internal grouting bolts as the core to provide support for the deep high-stress soft rock roadway. Huang et al. [10] took the engineering geologic conditions of the deep bolt-grouting supporting roadway as the background and thoroughly studied the permeability evolution and seepage diffusion mechanisms of the bolt-grouting grout in the cracked surrounding rock. Zhang et al. [11] performed bolt-grouting supporting for the soft rock roadway of the wells with a depth of 1000 kilometers in Zhuji coal mine and verified the effect of lagging grouting. Liu et al. [12] effectively controlled the dropsical problem of the surrounding roadway in the geological anomaly zone with grouting technology. Li et al. [13] developed a hydrodynamic grouting model test bed of a quasi-three-dimensional fracture, and then established a hydrodynamic grouting model study on the water inrush of fractured rock masses and obtained the principle of rapid bleeding of sedimentation and the rule of sedimentary nuclear diffusion of a slurry, so the quantitative evaluation of slurry diffusion and plugging effect was realized. Based on the unsteady seepage formula, Sun et al. [14] deduced the basic differential equations of the slurry seepage, and the numerical values were discretized. He obtained the finite elemental model of calculating a slurry seepage and performed the calculation and analysis combined with the actual grouting project. These results not only enriched the grouting model of a roadway surrounding rock and the theory of grouting and control technology but also achieved remarkable economic and social benefits.

For a long time, scholars have researched various technologies to control the surrounding rock of the faulted roadway [15–20]; however, there are few studies on the supporting mechanisms of the fractured zone of the mining roadway passing through a water-rich fault zone. Also, most of the research uses an engineering analogy or directly relies on experience to control the deformation of the roadway's surrounding rock in the fault fracture zone by using bolt wire cable and shield, etc., and due to the low strength of the surrounding rock in the fault fracture zone, the developed joint fissures and anchor rod (rope) are unable to easily find a stable anchorage point, which produces a hidden danger for safe production of mines. Bolt-grouting supporting can not only improve the cohesion and internal friction angle of the rock mass, thereby increasing the strength of the rock mass, but also can use a slurry to seal cracks in the surrounding rock, reduce the water permeability of the cracked rock, and prevent the inrush of water into the mine [21–25]. Currently, several methods to verify the effectiveness of bolt-grouting supporting include onsite in situ testing, indoor analogue simulation, and numerical software simulation. The former two have been gradually abandoned due to their high cost and difficulty to control the flow of the slurry, allowing for numerical software simulation to be favored by more and more scholars [26–30]. Therefore, the support mechanism and control effectiveness of the bolt-grouting supporting are typically analyzed by numerical methods and other quantitative methods in the fractured zone of the mining roadway passing through water-rich fault, and this has important guidance for the control of surrounding rocks in the passing through water-rich fault in the mining roadway.

This paper takes the fractured zone of a mining roadway passing through the water-rich fault of the 15107 working surface within the Yuxing coal mine as a case study to detect the contained water of the roof surrounding rock near the fault fracture zone. Based on the test results of the mechanical properties of the water-rich surrounding rock, a corresponding numerical model of fluid-structure interaction was established. Furthermore, this paper analyzed the permeability coefficient, pore pressure, cracked water velocity, and deformation failure characteristics of the surrounding rock under the conditions of shield supporting and bolt-grouting supporting. This work provides important theoretical and practical significance for the prevention, prediction of burst water, and consolidation of the blocked off water under the condition of passing through water-rich fault in the mining roadway.

2. Project Overview

The coal seam of the 15107 working face of the Yuxing coal mine is 15# coal, and the average thickness of the coal seam is 4.15 m with a dip angle of 3–8°. The straight roof is the K_2 limestone, and the rock formation is hard with developed fractures. The rock thickness is 8 m~12 m. The baseplate is gray-black mudstone or silty mudstone with a low strength and consists of numerous mineral components such as smectite that can easily be deformed and damaged as they are softened with water. The working face uses the long wall coal mining method along the working face, with a length of 200 m and propulsion length of 900 m. The recoverable reserves are 920,000 tons. The working face adopts integrated mechanized coal mining technology, and the gob of the working face adopts whole caving method to deal with the roof. In the excavation process of the return airway and haulage gate, a normal fault with a gap of 3.7~2.0 m was found and is the central turnoff of the working face. The fault gap revealed by the return airway is 3.7 m. The haulage gate revealed two other faults, which are 2.2 m and 2.0 m, respectively, with a distance between the two faults of 7 m. The return airway fault is about 35 m ahead of the haulage gate. The schematic diagram of the fault distribution in the working face is shown in Figure 1.

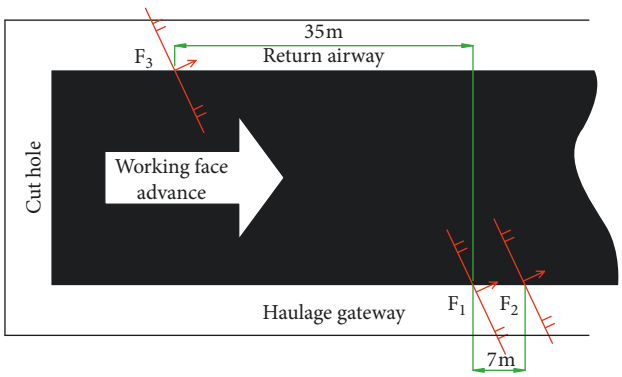

Figure 1: Fault distribution of the working face.

After the fault was found, the inflow of water in the roadway obviously increased, reaching 40 m^3/h. The aquifers that affect the 15107 working face during mining are mainly composed of fissure water in the 15# coal seams with the direct K_2 limestone roof and the water in the K_4 and K_5 limestone. Furthermore, the upper part of the 15107 working face is the old coal zone of the 3rd coal seam, and there is also excessive stagnant water. The water in the roof of the roadway enters the roadway along the cracks in the fracture zone, resulting in softening of the bottom mudstone and sandy mudstone and significantly reducing the strength of the mudstone, eventually leading to increased deformation of the roadway surrounding rock. The use of 16# ordinary I-beam steel erecting shield support and 12# mining I-beam steel erecting shield support for reinforcing a roadway in fault fracture zones cannot effectively control the stability of the roadway surrounding rock. This not only reduces the speed of the mining roadway and increases the cost of excavation but also allows a serious impact on the production and safety of the working face.

3. Transient Electromagnetic Method to Detect Water Source

A fault was encountered in the excavation process of the return airway and haulage gate, and the water inflow in the roadway suddenly increased after the fault was found. In order to prevent a water-bursting disaster caused by the fault connecting the water source in the upper part of the coal seam during roadway excavation to the advancing work surface, the water near the fault of 15107 working face was surveyed and drawn off, and the fault was grouted to block water sources. Using transient electromagnetic method of PROTEM47 to detect of 15107 return airway, a 300-meter-long survey line was arranged along the return airway. The starting point was about 50 m in front of the fault, and the measuring direction was divided into vertical direction and the direction of 45° toward the inner roof. The detection result is shown in Figure 2. A smaller area of the apparent resistivity chromatogram section (blue) indicates a higher water content in the region, while a larger region value (orange) indicates that the water content in the region is lower.

A total of two low-valued anomalies were detected in the vertical direction of the 15107 return airway (Figure 2(a)).

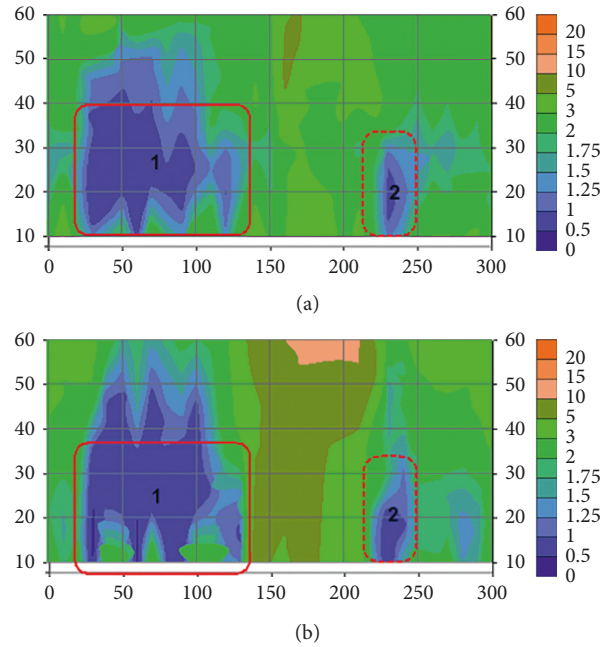

Figure 2: Apparent resistivity detected by the transient electromagnetic method in 15107: (a) apparent resistivity detected in vertical direction and (b) apparent resistivity detected 45° with the angle of the roof.

The number 1 abnormal area was located at stake number 30~130 m, and as inferred from the layer relationship, it was a relatively strong water-rich area near the roof of the fault fracture zone, located between 15 and 40 m from the tunnel roof. The number 2 abnormal area was located at the stake number 220~250 m, and as inferred from the layer relationship, it was relatively a less water-rich area of the roof rock compared to number 1. It was located between 10 and 25 m from the tunnel roof. The detection results in the direction of 45° toward the inner roof also found two low-value anomaly areas (Figure 2(b)), and the detection results correspond well with the vertical detection results.

Comparing the detection results in the different directions of the return airway, we found that the aquosity of the fault fracture zone was obviously stronger. This may be because the fault is a hydraulic connection with other aquifers or other sources of water, so that the area has a high water capacity. In the process of plugging the water of the roadway and face advance, we should timely grout the surrounding rock cracks so as to seal those also, while providing additional strength of support, and timely monitor the change of the inflow of the roadway and the deformation and damage of the surrounding rock.

4. Numerical Simulation of Roadway Grouting

4.1. Physical Mechanics Parameters of Surrounding Rock. The rock samples were taken from the roof and floor of the coal seam. Physical and mechanical properties were tested in their natural state in the laboratory. The uniaxial compressive strength of the K_2 limestone is 103.7 MPa, while the tensile strength is 13.8 MPa, classifying it as hard rock. The

floor of the coal seam is a black mudstone or silty mudstone, and its uniaxial compressive strength is 25.7 MPa, while the tensile strength is 2.13 MPa, which is classified as weak rock. There is a developed fracture within the fault fracture zone, and there is muddy cementation between the fractures, and the overall strength is low. After the fault was found, the water inflow in the roadway increased significantly, and the roadway surrounding rocks were softened after being immersed in water. Therefore, after soaking the rock samples of each rock formation in water for 6 hours, the mechanical properties of the rock samples were measured as shown in Table 1. But in the fault fracture zone, the rock samples could not be cored to produce rock samples, so the mechanical parameters were not determined.

As can be seen from Table 1, the mechanical parameters of the rock samples in different rock formations are weakened to different degrees as they absorb water, and among them, the baseplate mudstone and coal seam are the most obvious, with the strength decreasing by 17.46% and 32%, respectively, and the elastic modulus decreasing by 13.2% and 48.2, respectively.

4.2. Permeability Coefficient of Fractured Rock. Research [31–33] shows that water flowing through the fractured rock obeys Darcy's law, which can be expressed as

$$q = K_e J, \tag{1}$$

where q is the flow of single width fracture, m^3/s; K_e the permeability coefficient of fracture, $m{\cdot}s^{-1}$; and J is the pressure gradient.

Snow [34] simplified a crack into two parallel plates, and used the theory of fluid mechanics to derive the seepage equation within the fissure, which can be expressed as

$$q = \frac{ge^3}{12v} J, \tag{2}$$

where g is the acceleration of gravity, m/s^2; e is the fracture opening, m; and v is the kinematic viscosity coefficient, m^2/s.

Using Equations (1) and (2), the permeability coefficient of a single parallel fissure can be obtained as

$$K_e = \frac{ge^3}{12v}. \tag{3}$$

It is assumed that a single group of simple rock mass under uniaxial compression is as shown in Figure 3. The width of the unit is a, the length is b, the compressive load on the upper surface is σ_n, the average fracture spacing is l, and the average fracture opening is e. So, the total deformation of the rock mass element Δ_M, can be expressed as

$$\Delta_M = \Delta_R + N\Delta_F, \tag{4}$$

where Δ_R is the deformation of the rock; N is the total number of fracture in the unit; and Δ_F is the average deformation of each fracture.

Without considering the effect of gravity, the stress of rock and fracture is equal which can be expressed as

$$\sigma_n = E_n\varepsilon_n = \frac{E\Delta_R}{b} = k_n\Delta_F, \tag{5}$$

where E_n is the average elasticity modulus of rock mass; ε_n is the strain of rock mass; E is the average elasticity modulus of rock; and k_n is the fracture stiffness.

Through Equation (5), it can be solved as follows:

$$\Delta_R = \frac{bk_n\Delta_F}{E}. \tag{6}$$

It is also known that $\Delta_M = b\varepsilon_n$ and $N = b/l$ and taking them to Equation (4) can be expressed as

$$\Delta_F = \frac{\varepsilon_n l}{1 + k_n l/E}. \tag{7}$$

The initial opening of the fracture can be assumed to be e_0 as follows:

$$\begin{cases} \alpha = \dfrac{e_0}{l}, \\ \beta = \dfrac{k_n l}{E}, \end{cases} \tag{8}$$

where e_0 is the initial opening of the fracture.

Substitution of Equation (8) in Equation (7) yields Equation (9) as

$$\Delta_F = \frac{\varepsilon_n}{\alpha(1+\beta)} e_0. \tag{9}$$

When the strain of rock is ε_n, the fracture opening e is

$$e = e_0 - \Delta_F = \left[1 - \frac{\varepsilon_n}{\alpha(1+\beta)}\right] e_0. \tag{10}$$

By $\sigma_n = E_n\varepsilon_n$, the following is obtained:

$$e = e_0 - \Delta_F = \left[1 - \frac{\varepsilon_n}{\alpha(1+\beta)}\right] e_0 = \left[1 - \frac{\sigma_n}{E_n\alpha(1+\beta)}\right] e_0. \tag{11}$$

Substitution of Equation (11) in Equation (3) yields Equation (12) as

$$\begin{aligned} K_e &= \frac{g}{12v} e^3 = \frac{g}{12v} e_0^3 \left[1 - \frac{\sigma_n}{E_n\alpha(1+\beta)}\right]^3 \\ &= K_0 \left[1 - \frac{\sigma_n}{E_n\alpha(1+\beta)}\right]^3. \end{aligned} \tag{12}$$

4.3. Numerical Calculation Model. In order to seal the surrounding rock cracks of the fault fracture zone, prevent roof water from entering the roadway, and control deformation and damage of the roadway's surrounding rock, we took the geological condition of the return air laneway of the 15107 working face as background and established a fluid-structure interaction numerical model for the passing through water-rich fault in the mining roadway (Figure 4). The left and right boundaries in the model are the permeable boundary, and the fixed pore pressure of the fault fracture

Table 1: Mechanical parameters of rock strata.

Lithology	Elasticity modulus (GPa)	Poisson's ratio	Cohesion (MPa)	Internal friction angel (°)	Tensile strength (MPa)
K_2 limestone (natural state)	24.6	0.18	23.5	41	13.8
K_2 limestone (water-saturated state)	22.6	0.20	22.4	38	9.4
Coal (natural state)	3.26	0.28	6.3	28	2.7
Coal (water-saturated state)	2.83	0.3	5.3	27	2.1
Mudstone (natural state)	4.94	0.29	7.2	32	3.7
Mudstone (water-saturated state)	2.56	0.32	5.1	30	1.5

zone at the top boundary in the model was set to 1 MPa. The permeability coefficient of the rock formation was K_e according to the Equation (12), and the average fracture spacing was 10 mm and the average fracture aperture was 1 mm. The layer change due to fault throw was not considered here. We set the width of the fault fracture zone to 8 m, the dip angle to 75°, and the thickness of coal seam to 4 m. The model size was $60\,\text{m} \times 45\,\text{m} \times 45\,\text{m}$ (length × width × height). The roadway section was rectangular, the size was $4\,\text{m} \times 3\,\text{m}$, and the model was divided into 380,000 units.

In the roadway support structure, the 12# I-beam for mining used the beam elements model, and the rock bolt used the cable element model. The mechanical parameters of the I-beam and rock bolt are shown in Tables 2 and 3, respectively. Strain-softening model was used in the numerical simulation, and the surrounding rock parameters of strain-softening stage were obtained by the matching between numerical calculation model and the indoor test curve. In the calculation process, the elastic modulus, cohesion, and tensile strength of each rock layer were taken as 1/3~1/8 [35, 36] of the corresponding rock block mechanical parameters. Poisson's ratio of the rock body was taken as 1.2 to 1.4 times that of the rock mass, and the physical mechanics parameters of each rock layer are shown in Table 4. The top surface of the model was the stress boundary, the applied uniformly distributed load was $q = 7.5\,\text{MPa}$, the pressure measurement coefficient was 1.0, and the other boundaries had applied displacement constraints.

In the process of the numerical calculation, the choice of support modes was shield support and bolt-grouting support. This paper mainly discusses the permeability coefficient, pore-water pressure, fissure water velocity, and deformation law of the roadway surrounding rock under the condition of these two types of support modes. Grouting can not only improve the macroscopic mechanical properties of rock and largely decrease the softening coefficient of rock but also can greatly improve the physical mechanics properties of the fracture surface in fractured rock mass and improve hydraulic environment of the environment of rock mass, namely, the grouting effect in the surrounding rock. It is mainly reflected in two aspects [7]: reinforcing the surrounding rock and reducing the permeability of the surrounding rock. Therefore, the simulation of grouting in the bolt-grouting support was achieved by reducing the permeability coefficient of the surrounding rock and increasing the residual strength of the surrounding rock.

Qian et al. [4] studied the permeability coefficient, porosity, and the variation of compressive strength of the

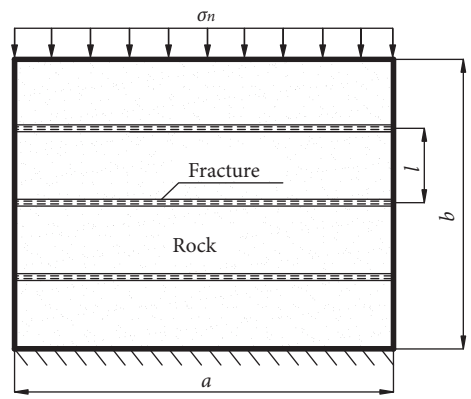

Figure 3: Simple rock unit with uniaxial compression.

model materials with different effective particle sizes and fineness modulus before and after grouting. The experimental results show that grouting significantly reduced the permeability of the material, and the permeability coefficient of each model decreased between 84% and 97%. The permeability coefficient of the rock mass after the grouting was 10% of the before grouting value. The effect of grouting to stabilize the surrounding rock was achieved by using the slurry to fill the rock fracture to consolidate the broken surrounding rock. The improvement of the mechanical properties of the fractured rock grouting after consolidation was expressed by the increase of the generalized cohesion and the generalized internal friction angle. The study showed that the residual strength of the rock can be increased by 0.7~2.0 times after grouting reinforcement with a general cement slurry [37–40]. The grouting reinforcement of the roadway at some point after excavation of the roadway is believed to be able to spread to the entire fracture zone of the surrounding rock. In the calculation process, the strength of the rock after grouting reinforcement was 1.5 times greater than before grouting.

4.4. Result and Analysis. The permeability coefficient variation curve of the roof surrounding rock under different supporting conditions is shown in Figure 5. Due to the existence of the fault fracture zone, the variation form of the permeability coefficient was a hump distribution, while the maximum permeability coefficient was in the fractured zone (the maximum of shield support was $9.996 \times 10^{-9}\,\text{m}\cdot\text{s}^{-1}$; the maximum of bolt-grouting support was $1.021 \times 10^{-9}\,\text{m}\cdot\text{s}^{-1}$). At the fault plane, the mutation rate was relatively quick (the two sides of the fault plane of the shield support were

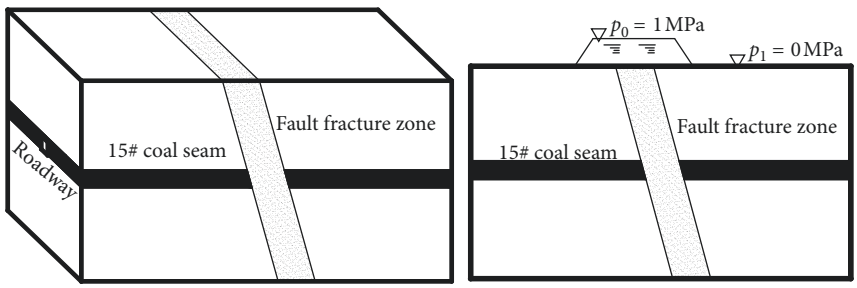

Figure 4: Numerical model of fluid-solid coupling in the roadway through fault.

Table 2: Mechanical parameters of 12# mining I steel.

12# mining I steel	Elasticity modulus (GPa)	Poisson's ratio	Yield strength (MPa)	Section area (m^2)	I_x (m^4)	W_x (m^3)	I_y (m^4)	W_y (m^3)
Beam unit	210	0.3	275	$3.97e^{-3}$	$0.867e^{-5}$	$0.145e^{-6}$	$0.178e^{-5}$	$0.375e^{-4}$

Table 3: Mechanical parameters of bolt.

Bolt	Elasticity modulus (GPa)	Poisson's ratio	Tensile load (t)	Section area (m^2)	Cement slurry stiffness on unit length (MPa)	Cohesive force of cement slurry in unit length ($N{\cdot}m^{-1}$)	Perimeter of outer ring of cement slurry (m)
Anchoring section					$1e^{10}$	$1e^{20}$	$8.792e^{-2}$
Free section	210	0.3	136	$3.799e^{-4}$	1	1	$6.91e^{-2}$
Grouting section					17.5	$20e^{4}$	$8.792e^{-2}$

Table 4: Mechanical parameters of each rock stratum in numerical calculation.

Lithology	Elasticity modulus (GPa)	Poisson's ratio	Cohesion (MPa)	Internal friction angel (°)	Tensile strength (MPa)
K_2 limestone	3.1	0.2	2.56	32	1.7
Coal	1.1	0.31	1.26	25	0.9
Mudstone	1.65	0.32	1.44	29	1.2
Fault fracture zone	0.85	0.32	1.02	26	0.85

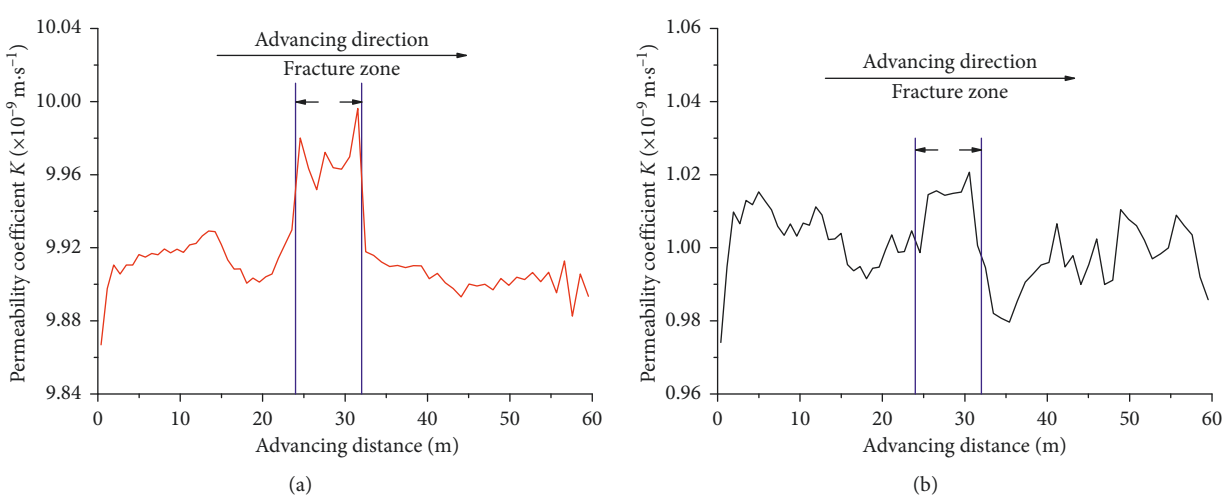

Figure 5: The permeability coefficient variation curve of roof surrounding rock under different supporting conditions: (a) shed supporting condition and (b) bolt-grouting supporting condition.

$0.05 \times 10^{-9}\,s^{-1}$ and $0.081 \times 10^{-9}\,s^{-1}$; the two sides of the fault plane of the bolt-grouting support were $0.016 \times 10^{-9}\,s^{-1}$ and $0.02 \times 10^{-9}\,s^{-1}$) because the surrounding rock fractures in the fault fracture zone were developed, and the permeability of the surrounding rock was relatively connected, and the stress concentration phenomenon occurs at the outer edge of the fault fracture zone, and the surrounding rock fractures closed under the high-stress conditions so that the permeability coefficient of the surrounding rock decreased. The impact range of the fault zone is about 20 m. In addition, due to the existence of faults and the difference in stress distribution of the surrounding rock in the excavation process, the permeability coefficient distribution outside the fault zone varied (the shield support was $9.883 \sim 9.929 \times 10^{-9}\,m \cdot s^{-1}$; the bolt-grouting support was $0.98 \sim 1.015 \times 10^{-9}\,m \cdot s^{-1}$). Under the two support conditions, the variation of permeability coefficient of the surrounding rock was similar, but after grouting with, the slurry flowed along the cracks of the fractured surrounding rock and filled the cracks in the surrounding rock after consolidation, so that the permeability coefficient of the surrounding rock was significantly reduced. The difference between the two reached a maximum near the fault fracture zone. At this time, the permeability coefficient of the surrounding rock with bolt-grouting support was 1/10 of that under the shield support. Therefore, grouting can effectively reduce the permeability coefficient of the broken surrounding rock, especially the permeability of the surrounding rock along the fault fracture zone, and prevent weakening of the surrounding rock caused by the massive influx of roof fissure water in the roadway, thereby improving the geomechanical environment in the surrounding rock of the roadway. Accordingly, in order to control the deformation of the roadway surrounding rock, the first step would be to block the fracture aisles of the surrounding rock in the roadway and reduce the permeability of the surrounding rock.

The pore-water pressure distribution in the fault fracture zone under different supporting conditions is shown in Figure 6. Under shield support, there was a significant decrease in the area of pore-water pressure around the roadway, but there was a relatively high pore-water pressure in the top roof, bottom roof of the roadway, and in front of the working face. This is because when the roadway was excavated to the fault fracture zone, deformation and damage occurred under the influence of the surrounding rock stress during the excavation process, which increased the permeability coefficient of the surrounding rock. The fissure water in the top roof crack flowed along the cracks and pores of the surrounding rock under the effect of pore-water pressure and then invaded into the roadway, causing the pore-water pressure around the roadway to decrease. The same conclusion can also be obtained from the velocity vector of the fissure water in the roadway section (Figure 7). Under of bolt-grouting support, the area of pore-water pressure around the roadway decreased, and the pore-water pressure in front of the bottom floor and working face essentially disappeared because during the grouting process the slurry flowed along the cracks of the fractured surrounding rock and filled the cracks in the surrounding rock after condensation, effectively reducing the permeability of the surrounding rock, thus preventing the continuous flow of top roof's fissure water into the roadway and surrounding rock of the bottom roof. The pore-water pressure in front of the bottom roof and the working surface was significantly reduced or reduced to zero.

Under different support conditions, the maximum displacement change of the roadway surface with the progress of the working face excavation in the roadway is shown in Figure 8. Before the heading face reached the fault fracture zone, the surrounding rock deformation of the roadway surface was small and changed little. When the heading face entered the fault fracture zone, the surface deformation of the roadway increased rapidly, and when the advancement of the working face went beyond the fault fracture zone, the maximum deformation of the surface continued to increase with the continued advancement. This is because as the working face entered the fault fracture zone, fissure water in the top roof flowed into the roadway, which resulted in the weakening of the surrounding rock. It causes continuous increase in the deformation of the surrounding rock. The use of bolt-grouting support not only changes the permeability of the surrounding rock and prevents the surrounding rock from being weakened by the fissure water in the roof but also improves the strength of the surrounding rock. Compared with shield support, the surface deformation of the roadway was reduced by 38.7%–65%. After the working surface surpassed the fault fracture zone, the performance gradually stabilized and effectively controlled the deformation of the fractured zone of the mining roadway, which provides the guarantee for the safe and efficient production of the mine.

5. Bolt-Grouting Supporting Scheme and Monitoring Results and Effects

In the vicinity of the fault, 15107 working face of the mining roadway adopted bolt-grouting combination support (Figure 9). The main technical parameters of the support were φ22 mm × 2400 mm regular screw-thread steel bolts, with seven bolts in the roof, and the interrow spacing was 700mm × 700mm. Each side was arranged with five bolts, and the interrow spacing was 800 mm × 700 mm. A steel ladder beam was welded with a φ10 mm steel. The top roof of the roadway was equipped with two high-strength cable supplement supports with the specification of φ15.24 mm × 7000 mm. The interrow spacing was 2100 mm × 2100 mm. The grouting bolt was a high-strength screw-thread steel grouting bolt with a specification of φ25 mm × 2500 mm and breaking force ≧ 15t. Four grouting bolts had been arranged on the roof with the interrow spacing of 1200 mm × 1400 mm, and three grouting bolts on each side with the interrow spacing of 1400 mm × 1400 mm. Among them, the bottom angle grouting bolt was arranged at an angle of 30° with the plane of the bottom roof. The grouting material was made of ordinary Portland cement additive. The cement adopted 525# ordinary Portland cement, the additive amount was 4%~6% of cement weight, and the water-cement ratio of slurry was 0.7 : 1~1 : 1; a cement additive of ACZ-1 was used at 4%~6% of cement

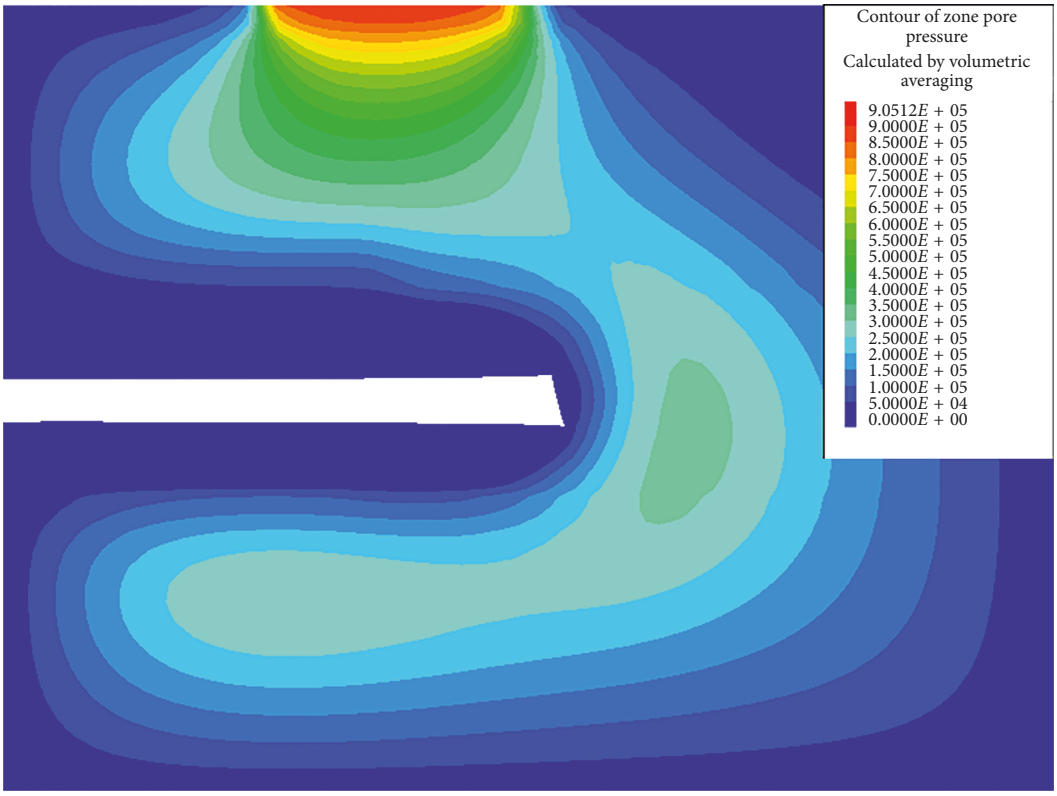

(a)

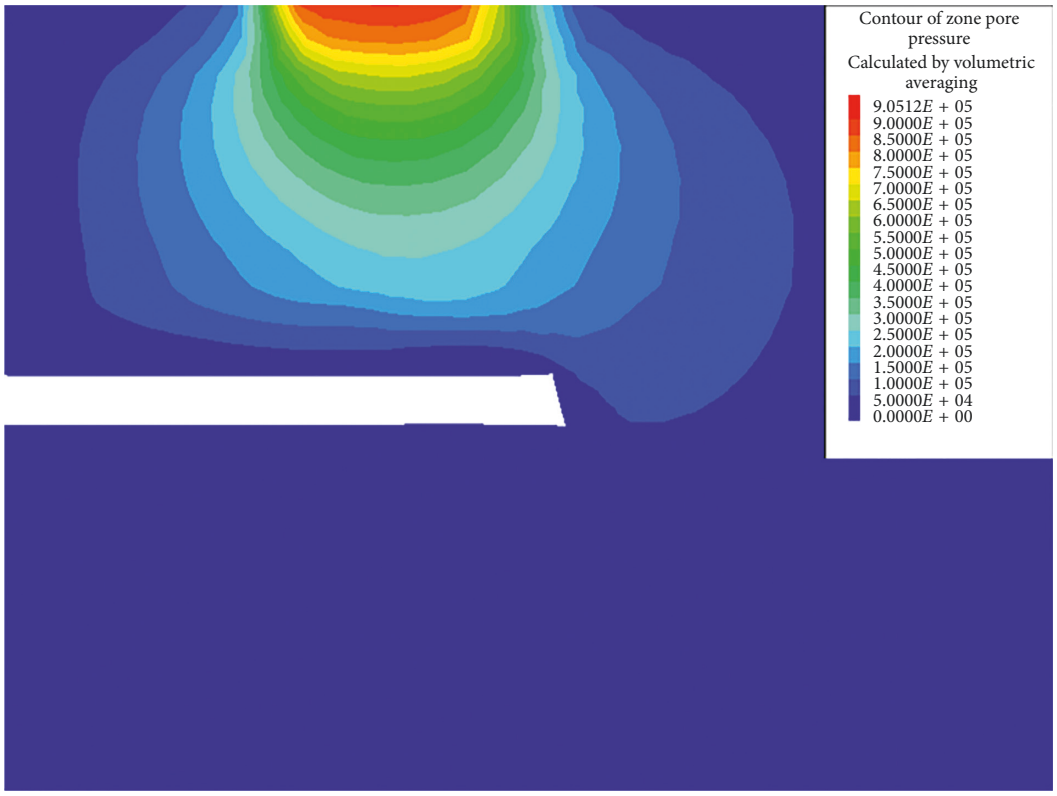

(b)

Figure 6: Pore-water pressure distribution in fault fracture zone under different supporting conditions. (a) Shed supporting condition and (b) bolt-grouting supporting condition.

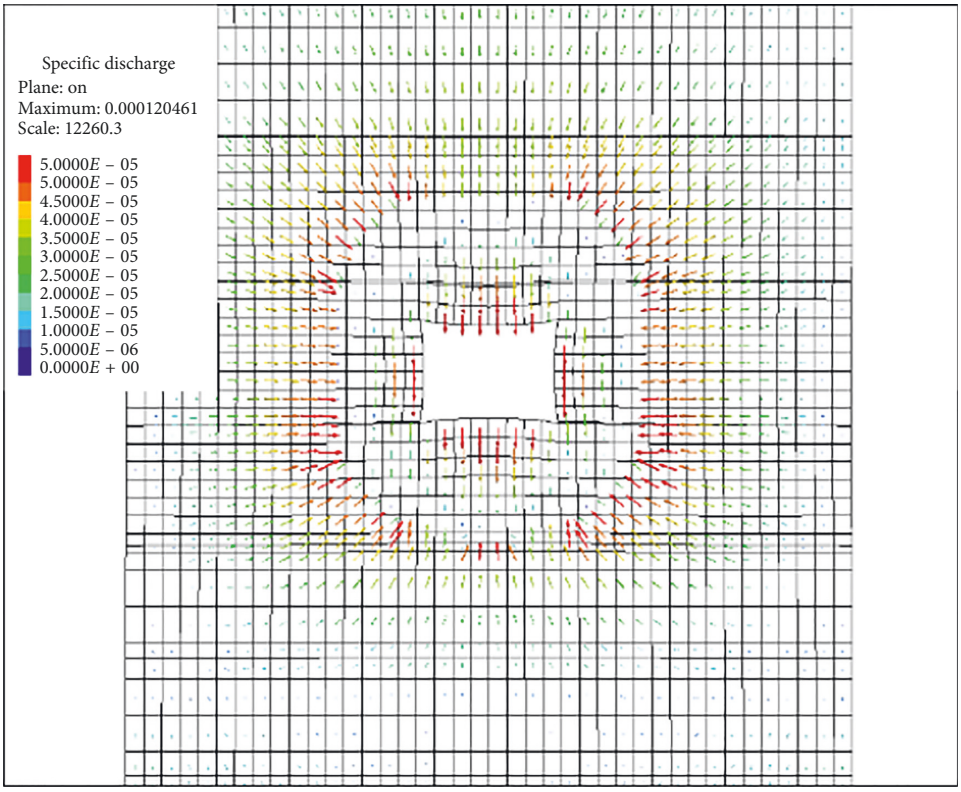

(a)

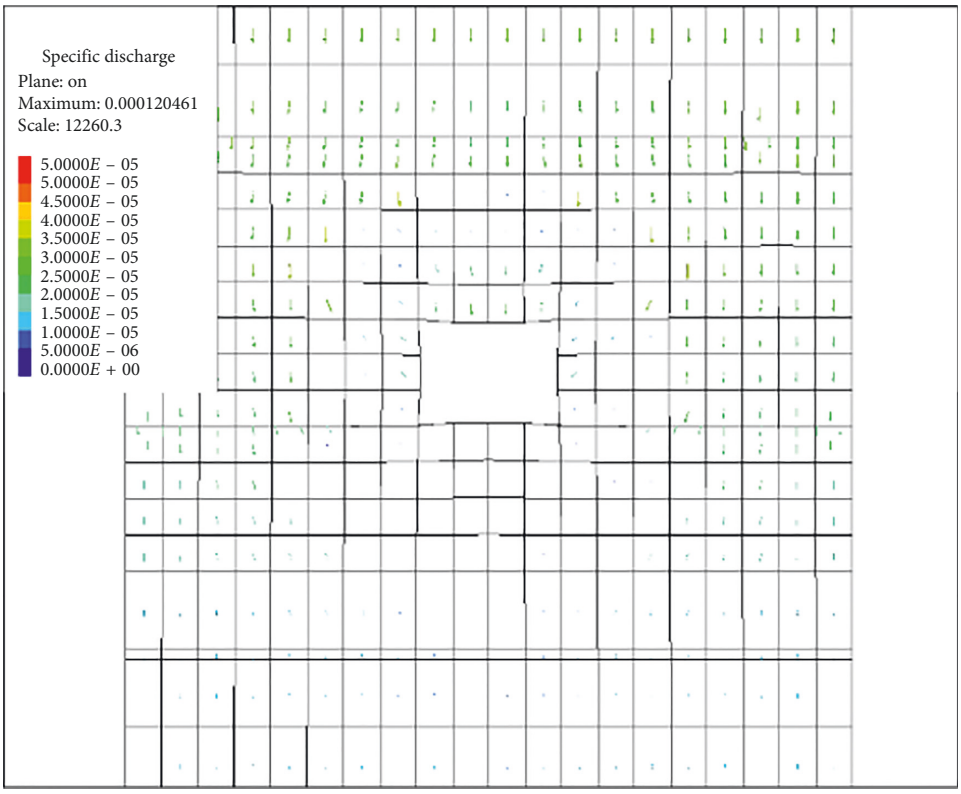

(b)

Figure 7: Flow velocity of fractured water in the fault fracture zone under different supporting conditions. (a) Shed supporting condition and (b) bolt-grouting supporting condition.

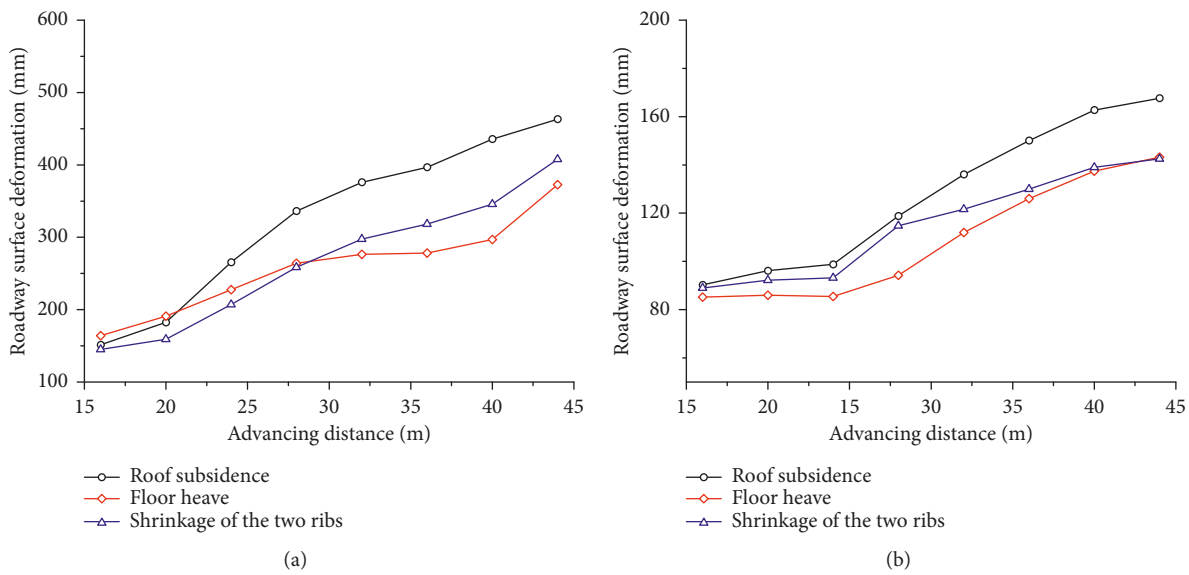

Figure 8: The maximum displacement's change of the roadway surface with the progress of the working face excavation: (a) shed supporting and (b) bolt-grouting supporting.

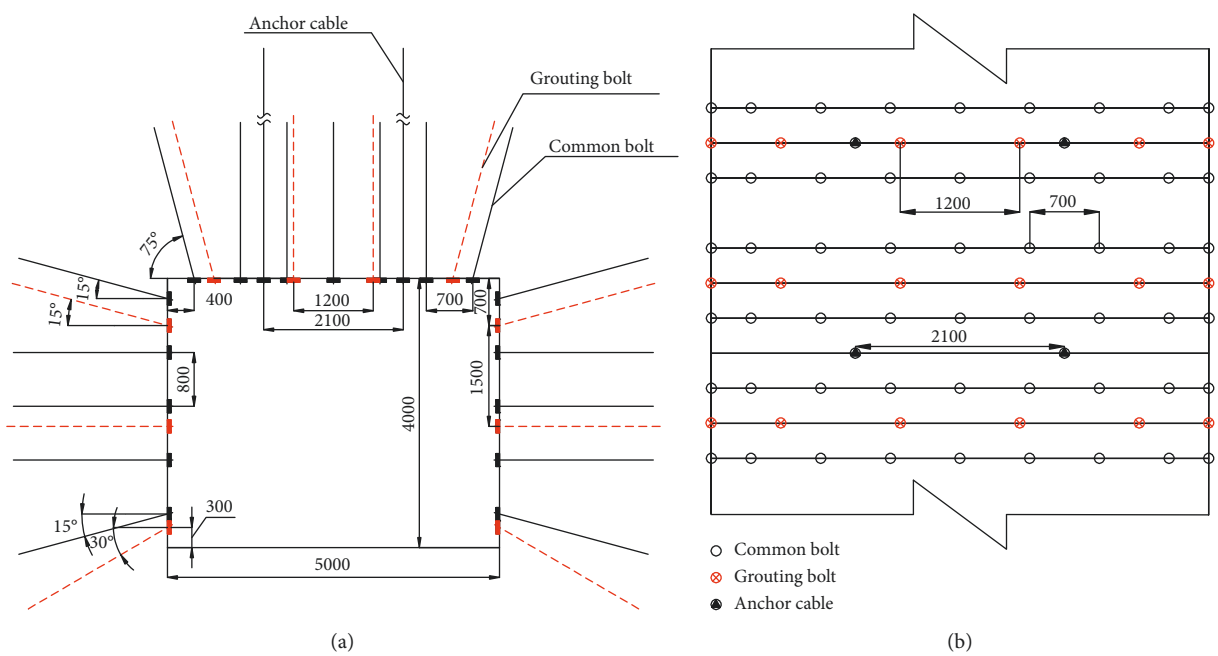

Figure 9: The scheme of bolt-grouting combined support: (a) roadway support section and (b) roadway support plane.

weight. The grouting pressure was 2.0~3.0 MPa with a maximum grouting pressure of 3.0 MPa for a time of 3~5 min per hole.

Displacement meters were installed within the roof, floor, and two ribs of the 15107 mining roadway to monitor deformation of the roadway surface. A monitoring station was set every 10 m, and a total of three monitoring sections were installed (Figure 10). The monitoring of the surface displacement of the roadway is shown in Figure 11. The deformation of the surrounding rock in the early excavation of the roadway rapidly increased (the maximum deformation rate between roof and floor was 17.2 mm/d; the maximum deformation rate between the two side ribs was 14.2 mm/d), and the surrounding rock velocity clearly decreased after grouting reinforcement. After 20 days, the deformation of the surrounding rock in the roadway gradually stabilized. The roof to floor convergence was 120~162 mm, and the rib to rib convergence was 104~140 mm. Deformation and damage after grouting to the surrounding rock were also effectively controlled.

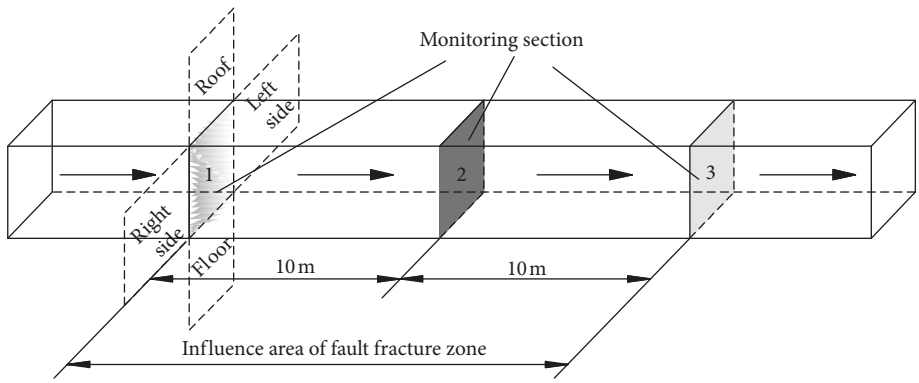

Figure 10: Layout of roadway monitoring section.

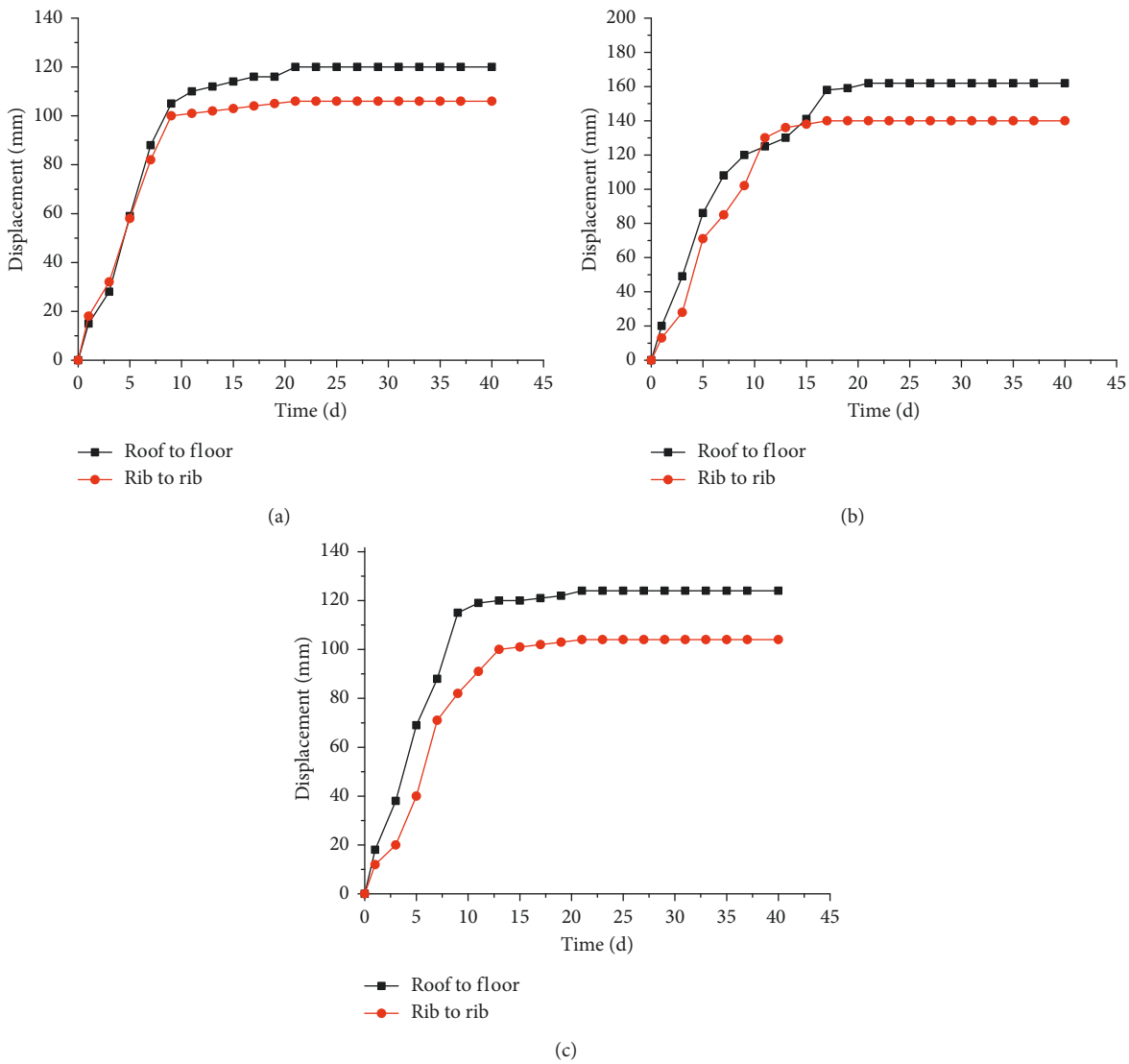

Figure 11: The surface displacement of the roadway: (a) monitoring station 1, (b) monitoring station 2, and (c) monitoring station 3.

At the same time, grouting also effectively reduced the water inflow near the fault zone, namely, reducing from the initial 40 m^3/h to 2~7 m^3/h. This is due to the fact that, after grouting, slurry filled the surrounding rock fracture near the fault fracture zone, and the solidified slurry effectively reduced the permeability of the surrounding rock in the area.

The fissure water cannot flow into the roadway through the original fissures, thereby effectively reducing the water inflow of the roadway.

Overall, bolt-grouting support not only effectively blocks the surrounding rock fracture near the fractured zone of the mining roadway passing through the water-rich fault, blocking the water inflow to the roadway, but also effectively controls the deformation of the surrounding rock in the fault fracture zone, ensuring the stability of the roadway's surrounding rock and safe production of the mine in the fractured zone of the mining roadway.

6. Conclusion

(1) Using the 15107 working face of the Yuxing coal mine which passes through a water-rich fracture zone, the transient electromagnetic method was used to detect the water content of the surrounding rock of the roof near the fault fracture zone. Between 15 and 40 m in the top roof of the fault fracture zone was a relatively strong area of water content. Therefore, in the advancing of the working face, we should timely grout to seal the surrounding rock fracture.

(2) Based on the test results of the mechanical properties of the surrounding rock in the state of natural and saturated, a numerical calculation model of fluid-solid coupling was established for the fractured zone of the mining roadway passing through a water-rich fault. We comparatively analyzed the permeability coefficient of the surrounding rock, the variation of pore pressure and fracture water velocity, and the deformation characteristics of the surrounding rock under the conditions of shield support and bolt-grouting support and can conclude the following.

Due to the existence of the fault fracture zone, the variation of the permeability coefficient is a hump distribution, with the maximum permeability coefficient in the fracture zone and along the fault section. The mutation rate is relatively quick. The impact range of the fault zone is about 20 m. The distribution of the permeability coefficient outside the fault zone fluctuates, and the bolt-grouting support effectively reduces the permeability coefficient of the surrounding rock, to 1/10 of that for shield support. Under the condition of shield support, there is a relatively higher pore-water pressure and larger fissure water velocity in the top roof, bottom roof of the roadway, and in front of the working face. Bolt-grouting support effectively prevents fissure water from inflowing into the surrounding rock of the roadway and bottom floor, so that the pore-water pressure in front of the bottom floor and the working surface is significantly reduced or even decreased to zero, and the fissure water velocity is also reduced. The self-bearing capacity of the confining pressure is improved by bolt-grouting support, which reduces the surface deformation of the roadway by 38.7%~65% compared to the shield support and effectively controls the deformation of the roadway surrounding rock.

(3) In the fault fracture zone along the roadway, the practice of bolt-grouting support was implemented, and the effect of water plugging and reinforcement after grouting was monitored. Results show that the bolt-grouting support not only effectively filled the surrounding fractures near the fractured zone of the mining roadway and blocked water gushing into the tunnel but also effectively controlled the deformation of the surrounding rock in the fault fracture zone, which ensures the stability of the roadway surrounding rock and the safe production of the mine when the mining roadway passes through the water enriched fault zone.

Data Availability

The data used to support the findings of this study are available from the corresponding author upon request.

Conflicts of Interest

The authors declare that there are no conflicts of interest regarding the publication of this paper.

Acknowledgments

This work was supported by the National Natural Science Foundation of China (Project nos. 51708245 and 51404245), the Natural Science Foundation for Colleges, Universities in Jiangsu Province (Project nos. 17KJB130003 and 17KJA560001), the Project with Science and Technology of Huai'an City (Project nos. HAG201606 and HAB201708), the Natural Science Foundation of Jiangsu Province (Project nos. BK20160426 and BK20170457), the Department of Education Foundation of Guizhou Province in China (Project no. QJHKYZ[2014]273), and the Cooperation Project with Science and Technology of Guizhou Province (Project no. QKHLHZ[2016]7047).

References

[1] M. G. Qian, J. L. Xu, and J. C. Wang, "Further on the sustainable mining of coal," *Journal of China Coal Society*, vol. 43, no. 1, pp. 1–13, 2018.

[2] H. P. Xie, F. Gao, and Y. Ju, "Research and development of rock mechanics in deep ground engineering," *Chinese Journal of Rock Mechanics and Engineering*, vol. 34, no. 11, pp. 2161–2178, 2015.

[3] M. C. He, "Progress and challenges of soft rock engineering in depth," *Journal of China Coal Society*, vol. 39, no. 8, pp. 1409–1417, 2014.

[4] Z. W. Qian, Z. Q. Jiang, L. W. Cao, and Q. Sun, "Experiment study of penetration grouting model for weakly cemented porous media," *Rock and Soil Mechanics*, vol. 34, no. 1, pp. 139–142, 2013.

[5] Y. Ju, Q. G. Zhang, Y. M. Yang, H. P. Xie, F. Gao, and H. J. Wang, "An experimental investigation on the mechanism of fluid flow through single rough fracture of rock," *Science China Technological Sciences*, vol. 56, no. 8, pp. 2070–2080, 2013.

[6] H. Y. Guo, X. Y. Lei, Y. M. Zhang, G. X. Yang, and Z. Niu, "Experimental research on hydrophilic characteristics of natural soft rock at high stress state," *International Journal of*

Mining Science and Technology, vol. 25, no. 3, pp. 489–495, 2015.

[7] Q. S. Liu, C. B. Lu, B. Liu, and X. W. Liu, "Research on the grouting diffusion mechanism and its application of grouting reinforcement in deep roadway," *Journal of Mining and Safety Engineering*, vol. 31, no. 3, pp. 333–339, 2014.

[8] L. G. Wang, M. Y. Li, and X. Z. Wang, "Study of mechanisms and technology for bolting and grouting in special soft rock roadways under high stress," *Journal of China University of Mining and Technology*, vol. 24, no. 16, pp. 2889–2893, 2005.

[9] L. G. Wang, Y. L. Lu, Y. G. Huang, and H. Y. Sun, "Deep-shallow coupled bolt-grouting support technology for soft rock roadway in deep mine," *Journal of China University of Mining and Technology*, vol. 45, no. 1, pp. 11–18, 2016.

[10] Y. G. Huang, L. G. Wang, and J. H. Zhang, "Reinforcement mechanism and slurry diffusion law of deep-shallow coupled fully bolting-grouting in deep broken roadway," *Electronic Journal of Geotechnical Engineering*, vol. 19, pp. 6319–6330, 2014.

[11] N. Zhang, B. G. Wang, X. G. Zheng, and X. L. Zhu, "Analysis on grouting reinforcement results in secondary support of soft rock roadway in kilometre deep mine," *Coal Science and Technology*, vol. 38, no. 5, pp. 34–38, 2010.

[12] K. D. Liu, Q. S. Liu, B. Liu, and Q. G. Gong, "Research on control measures and effects for roadway stability in geological anomaly zone," *Chinese Journal of Rock Mechanics and Engineering*, vol. 30, no. 12, pp. 2486–2497, 2011.

[13] S. C. Li, R. T. Liu, Q. S. Zhang, and X. Zhang, "Protection against water or mud inrush in tunnels by grouting: a review," *Journal of Rock Mechanics and Geotechnical Engineering*, vol. 8, no. 5, pp. 753–766, 2016.

[14] B. T. Sun, X. Z. Ling, C. Ling, and G. R. Zhu, "Numerical simulation for diffusion and pressure distribution of permeation grouting," *Journal of Hydraulic Engineering*, vol. 38, no. 11, pp. 1402–1407, 2007.

[15] D. Y. Qian, N. Zhang, D. J. Pan et al., "Stability of deep underground openings through large fault Zones in argillaceous rock," *Sustainability*, vol. 9, no. 11, pp. 2153–2181, 2017.

[16] Y. B. Li, "The integrated control countermeasures on floor heave of broken soft rock with high ground stress," *Advanced Materials Research*, vol. 875–877, pp. 2259–2263, 2014.

[17] X. G. Wang, K. Yuan, X. Z. Wu, and W. S. Zhu, "The study on the support technology of the soft rock roadway for coal mining under sea," *Applied Mechanics and Materials*, vol. 256–259, no. 1, pp. 1919–1922, 2013.

[18] L. M. Tian, B. Q. Yan, and J. H. Zhang, "Supporting reinforcement and stability analysis of the roadway crossing the fault in deep mining," *Revista Tecnica de la Facultad de Ingenieria Universidad del Zulia*, vol. 39, no. 10, pp. 222–228, 2016.

[19] Z. Z. Yuan, "Analysis of the large deformation mechanism of soft rock tunnel in great fault area and construction controls," *Electronic Journal of Geotechnical Engineering*, vol. 20, no. 25, pp. 12185–12193, 2015.

[20] R. Pan, Q. Wang, B. Jiang et al., "Failure of bolt support and experimental study on the parameters of bolt-grouting for supporting the roadways in deep coal seam," *Engineering Failure Analysis*, vol. 80, no. 10, pp. 218–233, 2017.

[21] J. H. Zhang, L. G. Wang, Q. H. Li, and S. S. Zhu, "Plastic zone analysis and support optimization of shallow roadway with weakly cemented soft strata," *International Journal of Mining Science and Technology*, vol. 25, no. 3, pp. 395–400, 2015.

[22] J. X. Liu, J. D. Jing, Y. Y. Feng, L. Wu, and P. S. Zhang, "Study on grouting anchor cable supporting technology of roadway through extra large fault fracture zone," in *Taishan Academic Forum-Project on Mine Disaster Prevention and Control*, pp. 114–118, Tai'an, China, 2014.

[23] J. H. Zhang, L. G. Wang, and B. Y. Jiang, "Bolt-grouting repair and reinforcement technology for damaged soft-rock roadway in deep mine," *Electronic Journal of Geotechnical Engineering*, vol. 19, no. Z7, pp. 18985–18995, 2014.

[24] Y. L. Chen, Q. B. Meng, G. Xu, H. S. Wu, and G. M. Zhang, "Bolt-grouting combined support technology in deep soft rock roadway," *International Journal of Mining Science and Technology*, vol. 26, no. 5, pp. 777–785, 2016.

[25] S. C. Li, H. T. Wang, Q. Wang et al., "Failure mechanism of bolting support and high-strength bolt-grouting technology for deep and soft surrounding rock with high stress," *Journal of Central South University*, vol. 23, no. 2, pp. 440–448, 2016.

[26] C. Zhao, B. E. Hobbs, A. Ord, P. Hornby, S. L. Peng, and L. M. Liu, "Theoretical and numerical analyses of pore-fluid flow patterns around and within inclined large cracks and faults," *Geophysical Journal International*, vol. 166, no. 2, pp. 970–988, 2006.

[27] J. H. Zhang, Y. Jiang, Y. Q. Fan et al., "Instability mechanism of surrounding rock of weakly cemented soft strata in shallow coal seam of west China," *Electronic Journal of Geotechnical Engineering*, vol. 22, no. 1, pp. 321–330, 2017.

[28] G. Y. Sun and X. Luo, "Numerical simulation analysis of different coal mine roadway support effect," *Advanced Materials Research*, vol. 807–809, pp. 2356–2360, 2013.

[29] Q. Wang, G. Chen, and E. D. Guo, "Nonlinear analysis of tunnels under reversed fault," *Indian Geotechnical Journal*, vol. 47, no. 2, pp. 132–136, 2017.

[30] A. J. Das, P. K. Mandal, R. Bhattacherjee, S. Tewari, and A. Kushwaha, "Effect of fault on the stability of workings underground extraction of coal," *Nexgen Technologies for Mining and Fuel Industries*, vol. 1, pp. 155–166, 2017.

[31] B. Nikbakhtan and M. Osanloo, "Effect of grout pressure and grout flow on soil physical and mechanical properties in jet grouting operations," *International Journal of Rock Mechanics and Mining Sciences*, vol. 46, no. 3, pp. 498–505, 2009.

[32] A. Varol and S. Dalgıç, "Grouting applications in the Istanbul metro," *Tunnelling and Underground Space Technology Incorporating Trenchless Technology Research*, vol. 21, no. 6, pp. 602–612, 2006.

[33] K. Kikuchi, T. Igari, Y. Mito, and S. Utsuki, "In situ experimental studies on improvement of rock masses by grouting treatment," *International Journal of Rock Mechanics and Mining Sciences*, vol. 34, no. 3-4, p. 594, 1997.

[34] D. T. Snow, "Ansisotropic permeability of fractured meida," *Water Resources Research*, vol. 5, no. 6, pp. 1273–1289, 1969.

[35] X. X. Chen, W. B. Xie, S. G. Jing, and W. Z. Wei, "Determination of mechanics parameters of mining induced rock mass for numerical simulation," *Journal of Mining and Safety Engineering*, vol. 23, no. 3, pp. 341–345, 2006.

[36] Y. X. Wang, D. B. Mao, and Q. X. Qi, "Research on determination of physio-mechanical coefficients during numerical simulation," *Journal of China Coal Society*, vol. 28, no. 6, pp. 593–597, 2003.

[37] Z. F. Li, S. C. Li, R. T. Liu, Y. J. Jiang, and F. Sha, "Model tests on grouting reinforcement of water-rich broken rock mass," *Chinese Journal of Rock Mechanics and Engineering*, vol. 36, no. 1, pp. 198–207, 2017.

[38] Y. L. Lu, L. G. Wang, B. Zhang, and Y. J. Li, "Optimization of bolt-grouting time for soft rockroadway," *Rock and Soil Mechanics*, vol. 33, no. 5, pp. 1395–1401, 2012.

[39] Y. F. Gao, Q. Z. Fan, and P. H. Wang, "Grouting reinforcement test of rock after peak value of strength and roadway stability control," *Rock and Soil Mechanics*, vol. 25, no. s1, pp. 21–24, 2004.

[40] M. R. Luo, "Grouting reinforcement technology for highway, bridge and tunnel engineering construction," *Boletin Tecnico/Technical Bulletin*, vol. 55, no. 4, pp. 169–176, 2017.

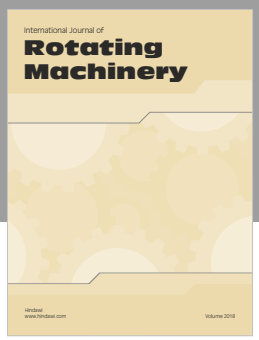

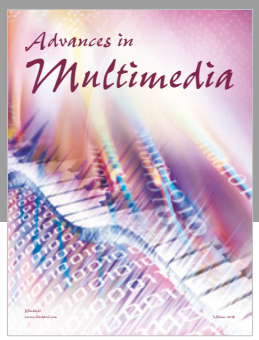

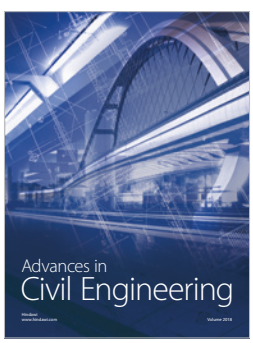

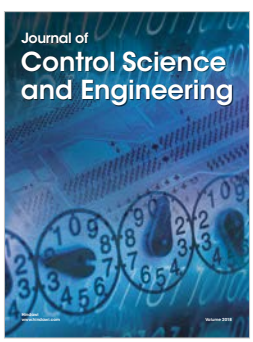

Hindawi

Submit your manuscripts at
www.hindawi.com